Solution Structure of Human Saposin C: pH-Dependent Interaction with Phospholipid Vesicles

Eva de Alba,* Solly Weiler,‡ and Nico Tjandra*

Laboratory of Biophysical Chemistry, National Heart, Lung, and Blood Institute, National Institutes of Health, 50 Center Drive, Bethesda, Maryland 20892

Received May 30, 2003; Revised Manuscript Received September 24, 2003

ABSTRACT: Saposin C binds to membranes to activate lipid degradation in lysosomes. To get insights into saposin C's function, we have determined its three-dimensional structure by NMR and investigated its interaction with phospholipid vesicles. Saposin C adopts the saposin-fold common to other members of the family. In contrast, the electrostatic surface revealed by the NMR structure is remarkably different. We suggest that charge distribution in the protein surface can modulate membrane interaction leading to the functional diversity of this family. We find that the binding of saposin C to phospholipid vesicles is a pH-controlled reversible process. The pH dependence of this interaction is sigmoidal, with an apparent pK_a for binding close to 5.3. The pK_a values of many solvent-exposed Glu residues are anomalously high and close to the binding pK_a. Our NMR data are consistent with the absence of a conformational change prior to membrane binding. All this information suggests that the negatively charged electrostatic surface of saposin C needs to be partially neutralized to trigger membrane binding. We have studied the membrane-binding behavior of a mutant of saposin C designed to decrease the negative charge of the electrostatic surface. The results support our conclusion on the importance of protein surface neutralization in binding. Since saposin C is a lysosomal protein and pH gradients occur in lysosomes, we propose that lipid degradation in the lysosome could be switched on and off by saposin C's reversible binding to membranes.

Saposin C is an activator of the lysosomal enzyme glucocerebrosidase that hydrolyzes the glycosphingolipid glucocerebroside to glucose and cerebroside (*1*). Mutations that affect the function of either the enzyme or saposin C cause Gaucher disease (*2*, *3*). This disease, with heterogeneous symptoms, results in sphingolipid accumulation in different human organs (*3*).

Saposin C belongs to a family of proteins whose amino acid sequences are related and therefore are supposed to share the so-called saposin fold. These proteins need to bind to membranes or lipids to carry out their different functions. It has been suggested that functional diversity possibly resides in their membrane-binding properties (*4*).

Saposin C is a glycoprotein with a single glycosylation site (Asn 22) to which N-linked oligosaccharides are covalently attached (*1*). Structural studies of the native glycosylated protein have shown oligosaccharides of different composition attached to the single glycosylation site, constituting a heterogeneous sample (*5*, *6*).

Biochemical assays indicate that glycosylated saposin C binds to membranes at acidic pH (*7*). Additionally, full activation of the enzyme glucocerebrosidase in vitro can only be achieved when saposin C is bound to membrane mimetics (*7*, *8*). Binding and activating sites of saposin C to the glucocerebrosidase have been identified in the presence of micelles (*9*).

Although the mechanism of activation of saposin C toward glucocerebrosidase is still unknown, a model has been proposed in which saposin C and the enzyme are bound to each other in the membrane where the sphingolipid is located (*10*, *11*).

According to many previously reported studies, the sugar moiety does not affect the function of saposin C (*12*) or its interaction with membranes. Similar binding and activating capacities of glycosylated and deglycosylated saposin C toward glucocerebrosidase indicate that the absence of the oligosaccharides does not produce any loss of protein activity (*9*). In fact, the nonglycosylated form seems to bind to the enzyme with slightly higher affinity. In addition, chemically synthesized saposin C displays 85% of the native biological activity (*13*), and both recombinant and natural saposin C activate glucocerebrosidase similarly (*14*). Nonglycosylated forms of other members of the family (saposins A and B) have the same activity toward their respective hydrolases as the glycosylated forms (*15*, *16*).

Furthermore, a previously reported study on saposin C's membrane association during its biosynthesis shows that membrane binding does not depend on the presence of N-linked oligosaccharides (*17*). The binding of saposin D to membranes is identical for both the glycosylated and the nonglycosylated forms (*18*).

To investigate the structural basis of the function of human saposin C and the factors that trigger membrane binding, we have determined its three-dimensional solution structure.

* Authors for correspondence: Nico Tjandra, Eva de Alba, e-mail: nico@helix.nih.gov, dealba@helix.nih.gov, phone: 301-402-3029, fax: 301-402-3404.

‡ Current address: GenPath Pharmaceuticals, 300 Technology Square, Cambridge, Massachusetts 02139.

10.1021/bi0301338
Published on Web 11/21/2003

The structure of saposin C compared to other saposin-fold family members provides an explanation for function variability of this protein family. In addition, we have studied by NMR[1] the changes in conformation and binding affinity to membranes as induced by pH. Our results provide structural insights into the mechanism of saposin C's interaction with membranes.

MATERIALS AND METHODS

Protein Preparation. Saposin C's DNA construct was prepared using PCR-based cloning to contain a thrombin cleavage site at saposin C's C-terminus. ^{15}N and ^{13}C isotopically enriched protein was expressed as a His-tagged protein in *Escherichia coli* strain BL21(DE3) using a pET-30b vector (Novagen) in minimal medium with ^{13}C-glucose and $^{15}NH_4Cl$ as sole carbon and nitrogen sources, respectively. The induction of protein expression was performed at 37 °C by the addition of 2 mM isopropyl β-D-thiogalactopyranoside for 4 h. Cells were harvested and resuspended in 100 mL of buffer containing 20 mM imidazole, 500 mM NaCl, 20 mM Tris, pH 8.0, lysozyme and serine protease inhibitor, 4-(2-aminoethyl)-benzenesulfonyl fluoride hydrochlorine. Cells were further lysed by ultrasonication and cleared by centrifugation. The supernatant was poured into a His-Bind resin (Novagen) and treated with biotinylated thrombin (Novagen) to cleave the histidine tag. The protein was further purified by reverse phase HPLC, then lyophilized and washed with HPLC grade water to eliminate residual salt. The construct for mutant saposin C (Glu 6 → Gln, Glu 9 → Gln) was prepared by PCR using the appropriately designed primers and saposin C's DNA construct as template. Expression and purification of the mutant protein were carried out identically to the native one. The amino acid sequence of saposin C and the mutant protein as determined by DNA sequencing is as follows:

Saposin C:

S_1DVYCEVCEF$_{10}$ LVKEVTKLID$_{20}$ NNKTEKEILD$_{30}$ AFDKMCSKLP$_{40}$ KSLSEECQEV$_{50}$ VDTYGSSILS$_{60}$ ILLEEVSPEL$_{70}$ VCSMLHLCSG$_{80}$ LVPR

Mutant:

S_1DVYC**Q**VC**Q**F$_{10}$ LVKEVTKLID$_{20}$ NNKTEKEILD$_{30}$ AFDKMCSKLP$_{40}$ KSLSEECQEV$_{50}$ VDTYGSSILS$_{60}$ ILLEEVSPEL$_{70}$ VCSMLHLCSG$_{80}$ LVPR

Residues 81−84 do not belong to the sequence of native saposin C but remain after thrombin cleavage of the His-tag.

NMR Data Collection for Structure Determination. NMR samples were prepared at ~1 mM protein concentration determined by weight of the freeze-dried protein. Protein solutions were extensively washed to remove residual salt. The pH was adjusted to 6.8 by adding small amounts of 0.1 M KOH and D_2O was added to 10% (v/v). Protein samples in fd phage (prepared as described; *19*) and Pf1 phage (ASLA) were prepared by mixing diluted solutions of phage and protein followed by concentration to ~0.8 mM protein and ~15 mg/mL phage.

NMR experiments were performed at 298 K on Bruker DRX 600 MHz and DRX 800 MHz spectrometers with triple resonance probes and tri-axial gradients. The combined information obtained from the experiments: ^{15}N-HSQC, ^{13}C-HSQC, sensitivity enhanced HNCO, CBCACONH, CBCANH, HBHACONH, HCCH-TOCSY (19.5 ms mixing time) was used to assign all backbone ^{15}N and ^{1}H amide chemical shifts and 100% of the ^{1}H and ^{13}C chemical shifts of amino acid side chains. Four-dimensional ^{15}N and ^{13}C-edited NOESY (120 ms mixing time) and ^{13}C-^{13}C-edited NOESY (120 ms mixing time) were used for NOE assignment. For a review on the different three- and four-dimensional ^{13}C and ^{15}N-edited NMR experiments for protein structure determination see Bax et al. 1993 (*20*). NMR experiments to measure residual dipolar couplings (*21*, *22*) were performed on the phage-containing samples. All NMR experiments were processed with NMRPipe (*23*) and analyzed with PIPP (*24*).

Backbone ^{15}N Relaxation Measurements. Relaxation experiments were performed with 0.25, 0.5, and 2 mM ^{15}N labeled human saposin C samples, pH 6.8 at 298 K on Bruker DRX 600 MHz. All data sets consisted of 128 × 512 complex data points that were zero-filled to 512 × 2048 data points. The ^{1}H carrier was positioned at the water frequency and the ^{15}N carrier at 116.5 ppm. States-TPPI quadrature detection in t_1 was used in all experiments (*25*).

The ^{15}N T_1 and $T_1\rho$ pulse sequences used (*26*) were modified to include the WATERGATE module (*27*), pulse field gradients (*28*), and a semiconstant time evolution period in t_1 (*29*). The $T_1\rho$ experiments utilized a continuous ^{15}N spin-lock (*30*) with a 2.5 kHz radio frequency field. $T_1\rho$ data were collected in an interleaved manner to minimize the effects of systematic errors. Four and eight scans were used for T_1 and $T_1\rho$ experiments, respectively. Relaxation times were calculated by fitting the dependence of the experimentally measured intensities with relaxation times to an exponentially decaying function. The relaxation times used in the $T_1\rho$ experiments were 3.7, 22.5 52.2, 82.5, 102.2, 122.3, 160.7, 202.5 ms and for T_1 experiments were 8, 32, 80, 176, 256, 400, 600, 800 ms.

^{15}N-^{1}H Heteronuclear NOE values were measured with a reported pulse program (*31*) and calculated from the ratio of peak intensities of experiments performed with and without ^{1}H presaturation. Sixteen scans per t_1 point were used. The total duration of ^{1}H presaturation was 3.76 s. NOE values were corrected as previously described (*31*) to compensate for errors caused by incomplete ^{1}H magnetization recovery.

Structure Calculation. Peak intensities from NOESY experiments were translated into a continuous distribution of interproton distances. A summation averaging $[(\sum r^{-6})^{-1/6}]$ was used to obtain distances from intensities. For the majority of the distances, an error of ± 25% of the distance was applied to obtain lower and upper limits. This error was increased to ± 35% for some distances that could be affected by spin diffusion processes. A modified version of the program X-PLOR (*32*) to incorporate dipolar couplings (*33*) was used for structure calculation. The fitting between the observed and calculated dipolar couplings was done using two different alignment coordinate systems, one for each set

[1] Abbreviations: NMR, nuclear magnetic resonance; HSQC, heteronuclear single quantum spectroscopy; NOE, nuclear Overhauser effect; NOESY, NOE spectroscopy; TOCSY, total correlation spectroscopy; TPPI, time proportional phase incrementation; RMSD, root mean square deviation; ppm, parts per million; HPLC, high-pressure liquid chromatography; PC, L-α-phosphatidylcholine; PS, L-α-phosphatidylserine; bis-ANS, 1,1′-bis(4-anilino)naphthalene-5,5′-disulfonic acid.

Table 1: Structural Statistics for the Solution Structure of Human Saposin C[a]

restraints	r.m.s deviations	
distances, Å (1806)	20 lowest-energy conformer	lowest energy conformer
sequential $\|i-j\| = 1$ (583)	0.032 ± 0.001	0.032
short-range $\|i-j\| \leq 5$ (673)	0.042 ± 0.001	0.041
long range $\|i-j\| \geq 5$ (550)	0.054 ± 0.001	0.054
hydrogen bonds, Å (28)	0.0439 ± 0.0006	0.0432
dihedrals, (°) (135)	0.93 ± 0.06	0.87
residual dipolar couplings, Hz (276)		
$^1D_{NH}$ (Pf1) (78)	0.84 ± 0.03	0.86
$^1D_{C\alpha C'}$ (Pf1) (66)	0.51 ± 0.01	0.51
$^1D_{C\alpha H}$ (Pf1) (74)	1.75 ± 0.08	1.78
$^1D_{NH}$ (fd) (58)	1.40 ± 0.40	1.00
deviations from idealized covalent geometry		
bonds, Å (1326)	0.0054 ± 0.0001	0.0054
angles (°) (2421)	0.88 ± 0.01	0.85
impropers (°) (627)	0.72 ± 0.02	0.71
structure quality		
Lennard-Jones[b] potential energy (Kcal mol^{-1})	-314 ± 8	-321
Ramachandran plot analysis[c]:		
residues 4−78	88.1%	86.1%
all residues (1−84)	84.7%	83.1%
coordinate precision[d]		
residues 4−78		
backbone (N, Cα, C′, O)	0.15 ± 0.02 Å	
all non-H atoms	0.77 ± 0.04 Å	
all residues (1−84)		
backbone (N, Cα, C′, O)	1.34 ± 0.34 Å	
all non-hydrogen atoms	1.87 ± 0.40 Å	

[a] The statistics were performed using the 20 conformers with the lowest overall energies. These conformers have no NOE or dihedral angle restraint violations greater than 0.4 Å and 4.5°, respectively. [b] The Lennard-Jones van der Waals energy was calculated with the CHARMM PARAM19/20 parameters and was not included in structure calculation. [c] Procheck (*81*) analysis for all residues gives 0.0% of the residues in a disallowed regions of the Ramachandran map. The percentages given account for residues in the most favored regions of the Ramachandran map. [d] The rmsd is reported between the 20 conformers and the mean coordinates by fitting all backbone heavy atoms.

of dipolar couplings. Initial values of the axial (D_a) and rhombic (R) components of the alignment tensors that are needed to do this fitting were calculated from the histogram distribution of dipolar couplings (*34*). Final values of D_a and R were obtained through a grid search by minimizing the total energy of the calculated structure. These are $D_a = 23$ Hz, $R = 0.31$ and $D_a = 16.6$ Hz, $R = 0.36$ for pf1 and fd phages, respectively. Residual dipolar couplings of NH, $C_\alpha H_\alpha$, and $C_\alpha C'$ bonds were used as restraints. A quadratic harmonic potential was applied for all dipolar couplings except those belonging to residues whose ^{15}N relaxation data indicate higher mobility than what is expected for secondary structure. In this case, a half-open square well penalty function was used (*22*).

Hydrogen bonds were defined according to the experimentally determined secondary structure of the protein. Two restraints were used per hydrogen bond (e.g., $r_{NH-O} = 1.5-2.5$ Å and $r_{N-O} = 2.4-3.6$ Å). The TALOS program (*35*) was used to obtain ϕ and ψ restraints only for those residues with statistically significant predictions.

pH Titrations. ^{13}C, ^{15}N-labeled saposin C and ^{15}N-labeled saposin C were dissolved in 90% HPLC grade water and 10% D_2O to form 0.5 mM samples in 0.5 mL total volume. The pH was adjusted by adding aliquots of 0.1 M NaOH and HCl stock solutions. The pH was not corrected for the isotope effect on the glass electrode. pH measurements were taken before and after each NMR experiment and the average of the two values was used for the analysis. The studied pH range was 7.36 to 4.22.

Analysis of pH Titration Curves. The pK_a values were determined from a nonlinear least-squares fit of the carboxyl ^{13}C chemical shift variation with pH of Glu side chains (*36*) to the Henderson−Hasselbalch equation. The errors in the obtained pK_a values were estimated by randomly adding to the experimental data, the error in chemical shift measurement obtained from reproducibility, and by refitting the new data. This procedure was done 10 times to estimate the error in the pK_a values as the standard deviation. The reported standard errors do not include uncertainty in the pH determination or other unknown potential systematic errors.

Vesicle Preparation. L-α-phosphatidylcholine from egg and L-α-phosphatidylserine from brain (Avanti Polar Lipids) in powder were dissolved in $CHCl_3$ and mixed to form a 4:1 molar PC:PS ratio. The $CHCl_3$ solution was dried overnight followed by speed-vacuum during 1 h. HPLC grade water was added to the mixture to form a 1 mM phospholipid solution that was equilibrated for 1 h. The solution was vortexed for 10 min and sonicated for 20 min in a bath sonicator. The temperature of the bath was controlled to avoid overheating.

Protein-Vesicle Binding Studies. Solutions of saposin C and the saposin C mutant at 1 mM concentration, pH 6.8, were mixed with solution of phospholipid vesicles (1 mM total lipid concentration) to form 0.5 mM protein/ 0.5 mM total lipid mixtures. The pH was adjusted to the desired values by adding sub-microliter volumes of 0.1 M solutions of KOH or HCl. NMR spectra (^{15}N-HSQC experiments) were acquired at the different pH values. The integral of the first t_1 point of the spectrum recorded at the highest pH value, which corresponds to a one-dimensional spectrum of the amide region of the protein, was calibrated to 100% of signal intensity. The same experiment performed in the absence of

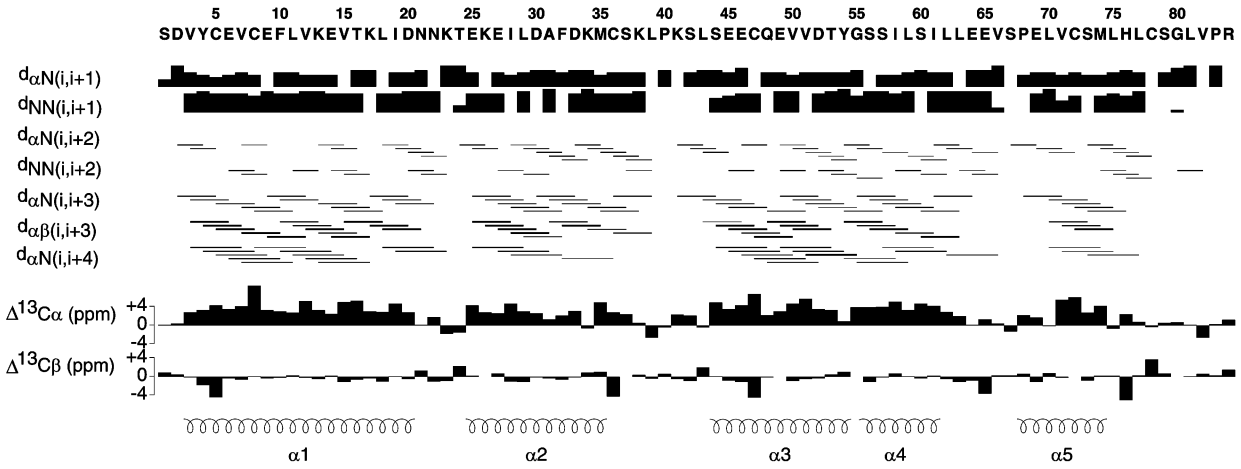

FIGURE 1: Summary of sequential and medium-range NOEs and ^{13}C secondary chemical shifts of human saposin C. The amino acid sequence and the secondary structural elements of the protein are shown in the upper and bottom parts of the figure, respectively.

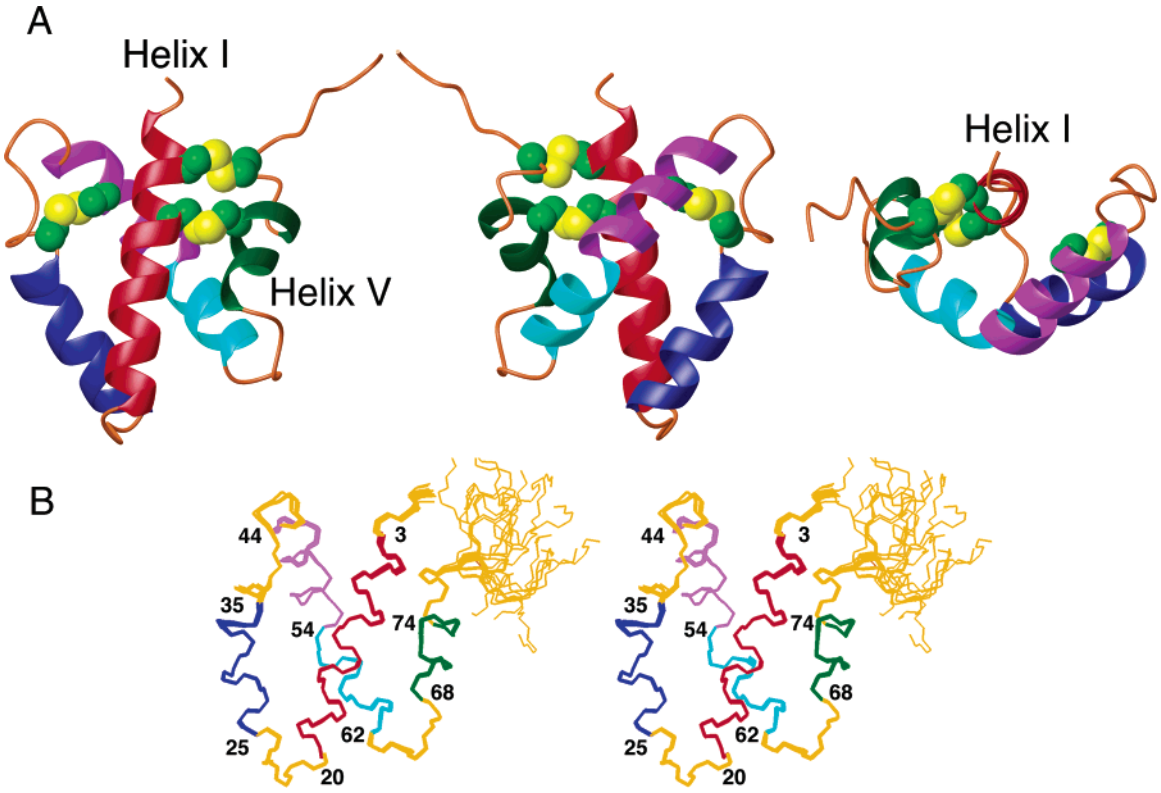

FIGURE 2: (A) Three different views of a ribbon diagram of human saposin C. Sulfur atoms of disulfide bridges are shown in yellow. (B) Stereoview superposition of 20 lowest-energy conformers of human saposin C. α-helices are color-coded. Helix I (red), helix II (dark blue), helix III (magenta), helix IV (light blue), helix V (green). α-helical starting and ending residues are labeled. Figure 2 was generated using the program MOLMOL (*82*).

vesicles at identical protein concentration and pH yield the same value for the integral of signal intensity. The intensity of the first t_1 point of the rest of the spectra recorded at different pH values was referenced to the point with 100% signal intensity. All measurements were repeated twice, and the reported values are the average of the two measurements. The measurement errors are represented in the corresponding figures.

RESULTS

Solution Structure of Human Saposin C. The NMR solution structure of human saposin C has been determined using distance restraints derived from Nuclear Overhauser effects and residual dipolar couplings measured in bacteriophage media. The combined structural information obtained from NOEs and dipolar couplings resulted in a high precision ensemble of structures (RMSD of 0.15 Å for the backbone atoms of the structured regions) (Table 1). The $^{13}C_\alpha$ secondary shifts (*37*) as well as short- and medium-range NOEs (*38*) indicate that the structure is mainly α-helical with short loops connecting the helices (Figure 1). The saposin C fold comprises five α-helices (Figure 2A,B). Helices III and IV could be considered to form a continuous helix containing a bend at residue Tyr 54 (Figure 2A). By grouping helices III and IV into one helix the saposin C fold can be described as a distorted four-helix bundle. The four

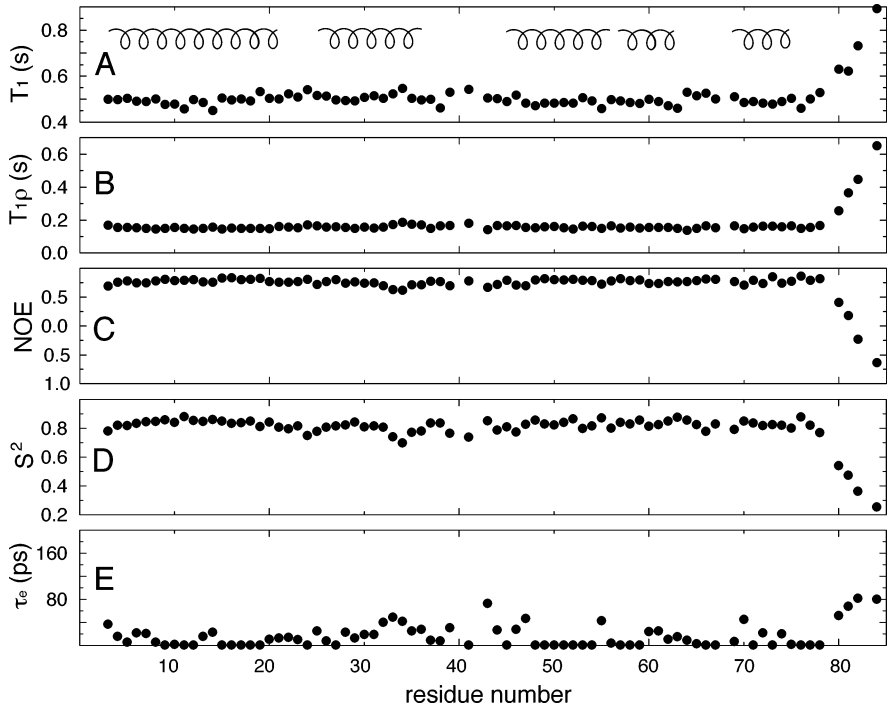

FIGURE 3: Backbone amide ^{15}N relaxation data for human saposin C at 0.25 mM. (A) Longitudinal T_1 relaxation times. (B) Transverse $T_{1\rho}$ relaxation times. (C) [^{1}H]-^{15}N Heteronuclear NOE. (D) Lipari-Szabo order parameters (S^2). (E) Time constants (τ_e). The secondary structural elements of the protein are shown in the upper part of the figure.

helices do not run antiparallel to each other, but helices II, III, IV, and V are packed against helix I forming half a sphere (Figure 2A). The structure of saposin C contains numerous hydrophobic contacts between the α-helices and three disulfide bridges connecting helices I and V (Cys 5−Cys 78, Cys 8−Cys 72), and the loop between helices II, III with helix III (Cys 36−Cys 47) (Figure 2A). The presence of three disulfide bridges could explain the large number of observed NOEs for a protein of the size of saposin C (Table 1). The oxidized state of the six Cys residues was clearly indicated by the ^{13}C chemical shift of their C_β atoms (Figure 1) (*39*). The corresponding pairs of Cys residues forming three disulfide bridges could be unambiguously identified from NOE data. Numerous NOEs were observed between Cys 36 and Cys 47, indicating the presence of a disulfide bridge between them, while neither was involved in NOE contacts with any of the other Cys residues. NOEs between Cys 5 and Cys 8 correspond only to the typical NOEs characteristic of α-helices (both Cys residues belong to helix I) and these are, C_αH-NH (i, i+3) and C_αH−C_βH (i, i+3) (Figure 1) (*38*). On the other hand, the large number of NOEs between Cys 78−Cys 5 indicate that these residues form a disulfide bridge. The third disulfide bridge involves Cys 72 and Cys 8, indicated as well by the presence of NOEs connecting them. Confirmation of this assignment comes from previous localization of saposin C's disulfide bridges using mass spectrometry (*40*).

NMR relaxation measurements can give information about protein dynamics (*41*). ^{15}N NMR relaxation of saposin C's backbone reveals a high degree of mobility at the N- and C-termini. Even the short loops that connect the α-helices of saposin C have a degree of mobility comparable to that of regular secondary structural elements (Figure 3). The Lipari-Szabo model-free formalism (*42*, *43*) was applied to obtain order parameters (S^2) and time constants (τ_e) (Figure 3). The slight decrease in the heteronuclear NOE from residue 32 to 35 may be related to fast backbone motions of large amplitude as indicated by the lower values of the order parameter in this region (Figure 3). By assuming fully anisotropic diffusion the calculated correlation time (τ_c) is 4.56 ns at a protein concentration of 0.25 mM. The rhombicity of the inertia tensor calculated from the structure is within 5% of that of the diffusion tensor obtained from the relaxation data. If assuming axially symmetric diffusion the principal axis of the inertia and diffusion tensors are within a solid angle of 15°. The analysis of ^{15}N relaxation data at 0.25 and 0.5 mM reveals that aggregation is minimal in this concentration range. An upper limit of ∼7% dimer is calculated with a monomer−dimer equilibrium model in which both species are considered spherical.

All charged amino acid side chains in saposin C are solvent exposed, while hydrophobic residues are partially or totally buried in the protein core (Figure 4A). The high content of negatively charged residues in saposin C (see protein amino acid sequence in Materials and Methods) and their location in the protein exterior are responsible for an electrostatic surface with a predominant negative potential (Figure 4A). Exposed hydrophobic surface is practically nonexistent. The few isolated positively charged features correspond to solvent exposed Lys residues (Figure 4A).

The coordinates of the ensemble of 20 structures calculated for human saposin C, the list of experimental NMR restraints, together with ^{1}H, ^{15}N, and ^{13}C chemical shift assignments have been deposited in the Protein Data Bank with accession code 1M12.

Conformational Behavior of Saposin C with pH. Previously reported studies show that saposin C binds to phospholipid vesicles at pH 5.0, while at pH close to 6.0 binding is not observed. The amount of protein bound to vesicles depends on vesicle composition (*7*). In addition, it has been

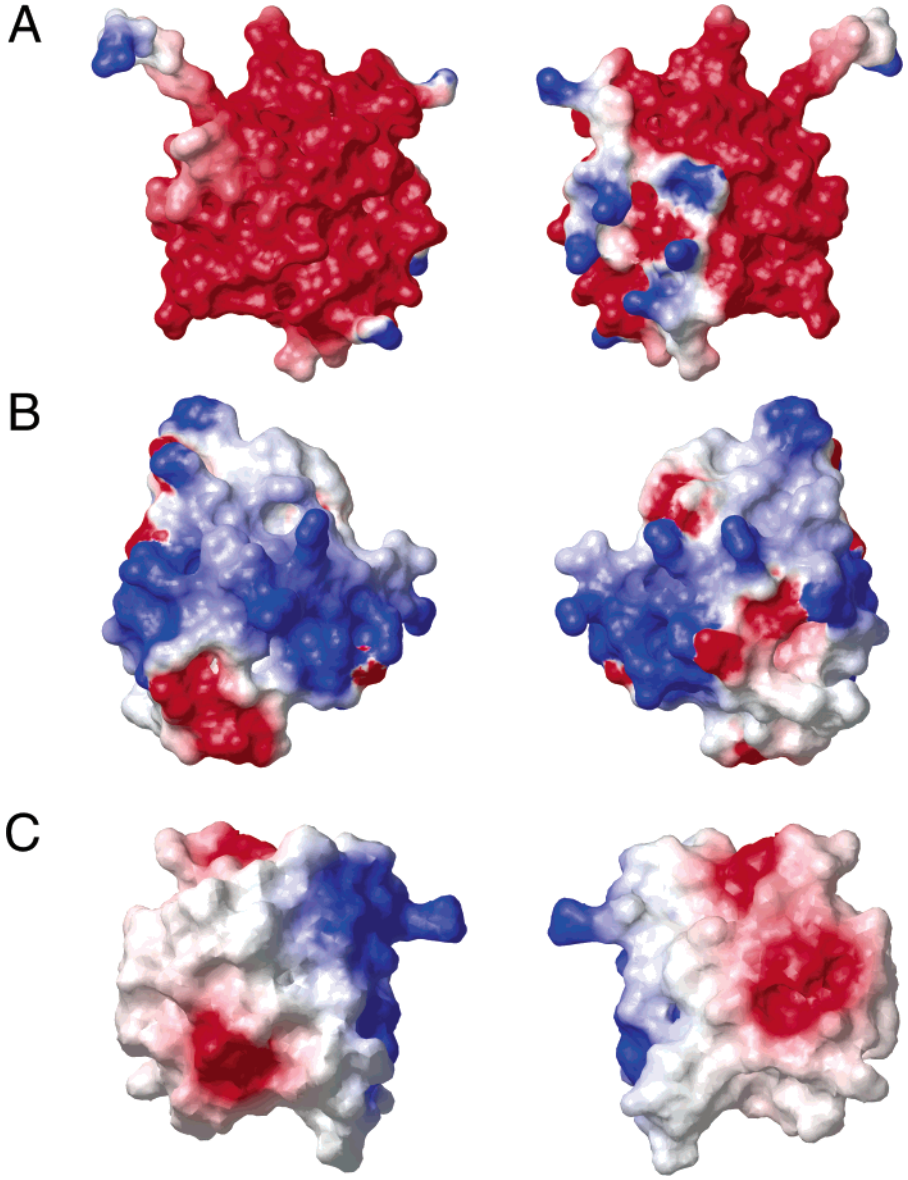

FIGURE 4: Front and back views of the electrostatic surface of (A) human saposin C, (B) NK-lysin, and (C) the saposin-like domain of plant aspartic proteinase prophytepsin. The views for the three proteins are equivalent in terms of the orientation of protein backbone. Figure 4 was generated using the program MOLMOL (*82*).

shown that the fluorescence intensity of the hydrophobic probe bis-ANS in the presence of saposin C increases as a function of pH. This result has been interpreted as a low pH-induced conformational change in saposin C that exposes hydrophobic areas to the solvent. It has been suggested that these hydrophobic regions are responsible for the binding of saposin C to membranes at acidic pH (*8*). To gain information concerning this potential conformational change at the residue level, we have studied the behavior of saposin C by NMR as a function of pH.

^{1}H and ^{15}N chemical shift changes of an^{15}N-HSQC spectrum (*44*−*46*) are used to identify the presence of conformational or chemical changes at the residue level upon the modification of solution conditions such as pH, or the addition of protein ligands. This technique has been extensively used to identify binding between proteins and ligands and to localize ligand-binding sites (*47*).

Superimposition of the ^{15}N-HSQC spectra of saposin C at pH 6.8 and 5.4 (Figure 5A) reveals slight chemical shift changes of only a few amide NMR signals. Signal linewidths do not change, which indicates that protein aggregation caused by pH decrease does not occur. The majority of the amide ^{15}N chemical shift differences observed upon solution acidification in a larger pH range (pH 6.8 to 4.2) are smaller that 1 ppm, and those that are larger correspond to amides of Glu or Asp residues whose side chains can titrate in this pH range (Figure 5B).

We have measured the pK_a values of 8 out of the 11 Glu residues present in the amino acid sequence of human saposin C (Figure 6). The carboxyl ^{13}C chemical shift dependence of Glu side chain with pH follows the classical sigmoidal Henderson−Hasselbalch behavior, suggesting that the titration of the side chain carboxylate group is responsible for chemical shift change with pH. Six out of the 11 Glu residues have a pK_a of ∼5.5 (i.e., approximately one pH unit above the value expected for an isolated Glu amino acid) (*48*). Two Glu residues have a pK_a value close to 5.1. Values of the pK_a lower than 4.9 could not be determined due to the acid-induced unfolding of saposin C at pH < 4.1.

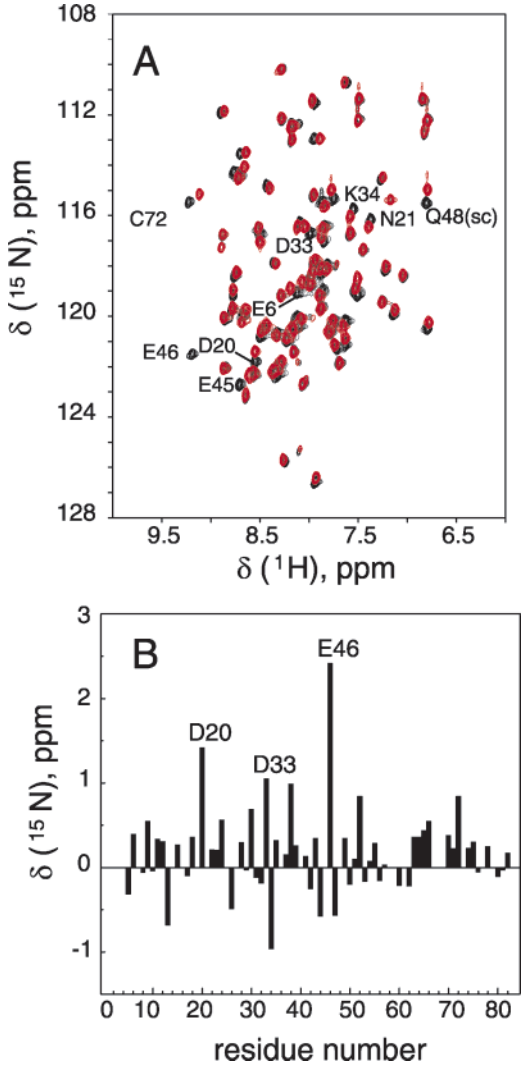

FIGURE 5: (A) ^{15}N-HSQC spectrum of human saposin C at pH 6.8 (black) and pH 5.4 (red). (B) Amide ^{15}N chemical shift differences of human saposin C between pH 6.8 and 4.2 versus residue number. Residues with largest chemical shift differences are labeled in both figures.

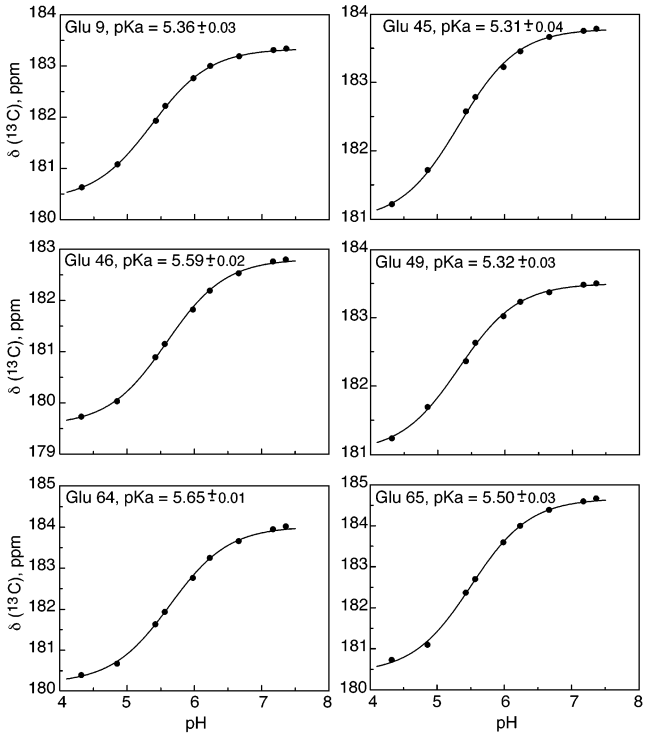

FIGURE 6: Titration curves of carboxyl ^{13}C chemical shifts of Glu residues' side chains of human saposin C with pH. pK_a values were calculated by a nonlinear least-squares fit of the experimental curve to the equation: $\delta_{obs} = [\delta_1 + \delta_2 \times 10^{(pH-pK_a)}]/[1 + 10^{(pH-pK_a)}]$ (δ_2 is the chemical shift value at the highest pH). pK_a values and errors are shown.

Glu residues with elevated pK_a values are located in three clusters in the protein surface: Glu 6−Glu 9, Glu 45−Glu 46−Glu 49, and Glu 64−Glu 65. Glu residues with more standard pK_a values tend to appear isolated in the protein structure. The pK_a values of isolated Glu and Asp amino acids in solution can change significantly by the presence of electrostatic interactions, hydrogen bonds, ionic strength, and exposure to solvent (*49*, *50*). In addition, it has been reported that anomalous pK_a values can be correlated with weak protein self-association processes ($K_d = 3-6$ mM) (*51*, *52*). pK_a variations of ~ 0.3 pH units have been attributed to this effect (*51*, *52*). ^{15}N relaxation data of saposin C indicate that <7% dimers are present at 0.5mM (the concentration used to measure the pK_a values). Therefore, it is expected that self-association may have only a minimal effect in the anomalously high pK_a values of saposin C's Glu residues.

Since the hydrophobic residues of saposin C are totally or partially buried in the protein core (Figure 4A), the exposure of patches of hydrophobic surface would very likely imply a large conformational change upon solution acidification. The almost identical ^{15}N-HSQC spectra of saposin C at pH 6.8 and 5.4 suggest that such conformational change does not take place.

The lack of ^{1}H amide chemical shift dispersion at pH lower than 4.1 indicates that saposin C is partially or totally unfolded under this condition, in agreement with data of bis-ANS binding (*8*).

Interaction of Saposin C with Phospholipid Vesicles and Triton X-100 Micelles. The binding of saposin C to negatively charged phospholipid vesicles as a function of pH has been studied by changes in NMR signal intensity. NMR signals broaden to the point of being unobservable when molecular tumbling is very slow. Vesicles, which can have an overall molecular mass larger than 100 kDa, tumble very slowly (*53*). Therefore, NMR signals that are observed in the presence of vesicles must belong to the protein that is free in solution. NMR signal intensity is proportional to the concentration of ^{1}H and ^{15}N amides of saposin C free in solution in our experiments. The NMR spectrum of saposin C does not change by the addition of vesicles at pH 6.8. In contrast, when the pH is decreased to 5.4, NMR signal intensity is reduced to ~64% (Figure 7A), indicating that approximately 36% of the protein molecules are bound to vesicles at pH 5.4. When the pH is increased back to 6.8, the signal intensity recovers to 91% of its original value (Figure 7A), reflecting the release of vesicle-bound protein back into solution and the reversibility of the binding process with pH.

No significant line broadening or chemical shift variations in the amide signals of saposin C's ^{15}N-HSQC spectrum at 0.5 mM protein concentration and pH 5.4 are observed by the addition of vesicles.

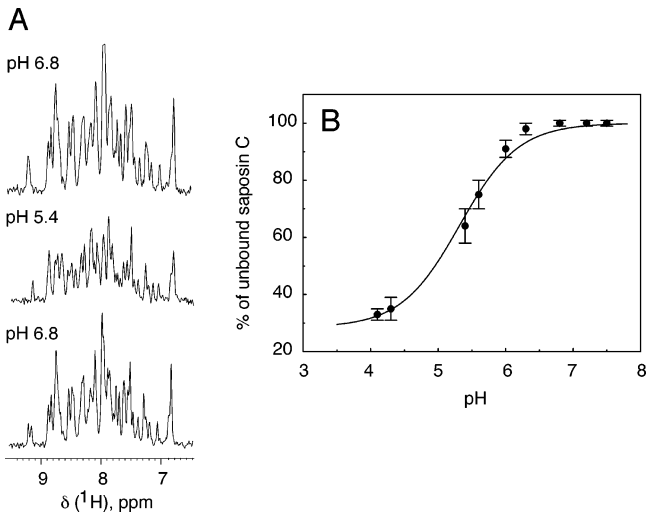

FIGURE 7: (A) One-dimensional projections of ^{15}N-HSQC spectra of saposin C (0.5 mM) in the presence of phosphatidylcholine (PC) and phosphatidylserine (PS) vesicles (0.5 mM total lipid concentration) at pH 6.8 (top), 5.4 (middle), and back to pH 6.8 (bottom) to demonstrate binding reversibility with pH. Percentage of proton population of the middle spectrum normalized with respect to the top spectrum is 64%. (B) Percentage of human saposin C free in solution in the presence of vesicles at different pH values as measured by NMR signal intensity (Materials and Methods). The data presented are an average of two measurements. Thin bars represent the error in the measurement. Binding studies were not performed between pH 5.4 and 4.3 because the protein precipitates in this pH range at a concentration of 0.5 mM. The continuous line represents the fitting of the experimental data to the Henderson−Hasselbalch equation.

Figure 7B shows that the pH dependence of saposin C's binding to vesicles does not follow a classical Henderson−Hasselbalch sigmoidal behavior. Nevertheless, in an attempt to obtain an apparent pK_a value for binding, the data were fitted to the Henderson−Hasselbalch equation resulting in an apparent pK_a value of ∼5.3 for protein-vesicle binding. This value is similar to the pK_a values of several saposin C's Glu residues (Figure 6), which suggests that neutralization of the side chains of these residues is an important factor for binding. The role of more than one titratable group in protein−vesicle binding could explain the observed non Henderson−Hasselbalch behavior. At the protein-to-lipid molar ratio at which the pH dependence of binding has been studied (0.5 mM protein/0.5 mM lipid), the amount of protein is in excess with respect to lipids and ∼33% of saposin C still remains in solution at the lower pH. Using higher lipid to protein molar ratios in sedimentation assays 100% binding has been observed (*7*).

A decrease in NMR signal intensity can result from protein aggregation or a change in protein dynamics. NMR relaxation data provide information on these processes (*54*). ^{15}N transverse relaxation time ($T_1\rho$) of 0.5 mM saposin C in the presence of vesicles at either pH 5.4 or pH 6.8 is in the range 145−153 ms. This value is similar to that obtained in the absence of vesicles at the same concentration ($T_1\rho \sim 140$ ms). This result indicates that the dynamic behavior of the protein free in solution is unmodified by the presence of vesicles at pH 5.4 or 6.8, and suggests that protein−vesicle binding is a slow process in the NMR time scale. It is important to mention that when the pH is decreased in the absence of vesicles no signal intensity change is observed. Therefore, the only possible explanation for signal intensity reduction upon pH decrease is that some of the protein that was free in solution in the presence of vesicles at pH 6.8 binds to the vesicles at pH 5.4, becoming undetectable by NMR.

To test the effect of electrostatic interactions in the binding of saposin C to negatively charged vesicles, 400 mM NaCl was added to the protein−vesicle mixture at pH 5.4, where binding occurs, and 6.8 (no binding). No increase or decrease in free-protein NMR signal intensity was observed at either pH (data not shown). Additionally, we studied the binding of saposin C to micelles formed by the noncharged surfactant Triton X-100 by NMR. Saposin C's ^{15}N-HSQC spectra are identical in the presence and absence of Triton X-100 at pH 6.8. In contrast, at pH 5.4, almost all NMR signals disappear (data not shown), reflecting the binding of saposin C to Triton X-100 micelles. When the pH is increased back to 6.8, all signals reappear and the spectrum looks identical to the original one, indicating that the interaction between saposin C and Triton X-100 is also reversible with pH.

Interaction of Mutant Glu 6 → Gln, Glu 9 → Gln Saposin C with Phospholipid Vesicles. We have designed mutations in saposin C to study the overall effect of side chain neutralization in the membrane-binding process controlled by pH.

Only two residues (Glu 6 and Glu 9) that titrate in the studied pH range were mutated to Gln, to avoid changes in protein structure, stability and solubility. The negative charge of the Glu side chain is no longer present in the Gln-containing mutant, which possibly implies a decrease in the negative charge of the electrostatic surface. The membrane binding studies of the mutant and wild-type proteins were performed at pH 4.3, where the plateau for maximum binding is reached and small differences in pH should not cause large differences in binding (Figure 7B). This pH was also chosen on the basis of the different pH ranges in which both proteins precipitate at the high concentrations required for the NMR studies (pH = 4.3−5.4 for saposin C and pH = 4.3−5.8 for the mutant). The mutant protein binds to phospholipid vesicles in a pH-controlled reversible process. At pH 4.3, ∼22% of the mutant is not bound to the membrane, while at the same pH 35% of saposin C remains free in solution (Figure 8A). The mutant protein binds to phospholipid vesicles to a greater extent at acidic pH than the wild-type does. One possible explanation for this difference in binding can be found in the pH titration curves of Glu 6 and Glu 9 (Figure 8B). At pH 4.3 the titration curves of Glu 6 and Glu 9 have not finished, which implies that native protein molecules have negatively charged side chain for Glu 6 (∼13%) and Glu 9 (∼8%). Since these residues were mutated to Gln, the mutant has neutral side chains in this region. Thus, at pH 4.3 a larger population of mutant protein has neutralized its surface, leading to a larger population of molecules that bind to the negatively charged phospholipid vesicles. It cannot be ruled out the possibility that the mutations to Gln may have modified the pK_a values of other Glu residues, therefore, changing the charge of the protein electrostatic surface which in turn may lead to a different binding affinity.

DISCUSSION

Interaction of Saposin C with Membranes. The interaction of saposin C with phospholipid vesicles and Triton X-100

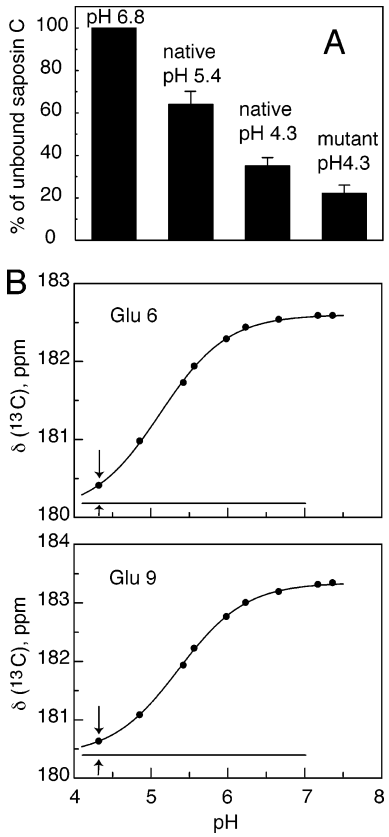

FIGURE 8: (A) Percentage of population of native and mutant proteins not bound to the vesicles at the different pH values. Thin bars represent the error in the measurement. (B) Titration curves of carboxyl ^{13}C chemical shift of Glu 6 ($pK_a = 5.12 \pm 0.02$) and Glu 9 ($pK_a = 5.36 \pm 0.03$) side chains with pH in human saposin C. Arrows provide an indication of the population of negatively charged Glu 6 and Glu 9 in native saposin C at pH 4.3.

is a reversible process dependent on pH (Figure 7A). The highly negatively charged electrostatic surface of saposin C at pH 6.8 (Figure 4A) prevents binding. This could be due to electrostatic repulsion toward the negatively charged vesicles or the high energetic cost of transferring protein negative charges from the polar aqueous environment to the apolar interior of the vesicle or micelle membrane. If the pH is decreased to 5.4, approximately 36% of the protein binds to phospholipid vesicles (Figure 7A) and protein−Triton binding also occurs. Many Glu residues in saposin C have pK_a values close to the apparent pK_a for binding (Figures 6 and 7). A pH decrease to 5.4 neutralizes ~50% of the side chains of these Glu residues by protonation, partially neutralizing in turn the electrostatic surface. In addition, NMR data indicate the absence of conformational changes when the pH is lowered from 6.8 to 5.4 (Figure 5A). One possible explanation for membrane binding triggered by pH decrease is the partial neutralization of the electrostatic surface of saposin C. Figure 7B shows that the pH dependence of saposin C's binding to vesicles does not follow a classical Henderson−Hasselbalch sigmoidal behavior, as expected when more than one titratable group with different pK_a values are involved in the binding process.

Our results regarding NaCl addition to protein−vesicles mixtures and the interaction of saposin C with the noncharged detergent Triton X-100 at acidic pH suggest that interactions with the membrane involve more than the polar heads of the phospholipids. In addition, these data suggest that binding is not impeded by electrostatic repulsion between saposin C and the negatively charges vesicles, but by the energetically unfavorable event of introducing a negative charge in an apolar environment.

We can safely rule out a critical effect of vesicle charge status on pH-dependent protein-binding in the studied pH range since PC and PS have phosphate groups with pK_a values close to 1 (*55*). In addition, the pK_a values of the amino and carboxylate groups of PS in PS/PC mixed vesicles have been reported to be 9.8 and 3.6, respectively (*56*). At the pH value that coincides with the binding pK_a (5.3) the percentage of lipid titratable groups that have began to titrate can be neglected. Additionally, the similar pH dependence in the binding of saposin C to the neutral detergent Triton X-100 indicates that membrane charge does not have a dominant role.

Although the binding of saposin C to phospholipid vesicles may follow a complex mechanism, in which possibly different events take place, a critical one seems to be the neutralization of the electrostatic surface. The binding behavior of the mutant protein in comparison to that of native saposin C (Figure 8) strengthens our conclusions regarding the key role played by the electrostatic surface of the protein in membrane binding.

The most probable mechanism for protein release from the membrane is based on displacement of two coupled equilibria. One equilibrium involves the unprotonated and protonated forms of the free protein in solution. The other equilibrium relates the protonated protein free in solution and bound to the membrane. When the pH increases, the larger concentration of hydroxyl ions should shift the first equilibrium toward the unprotonated form of the protein, this in turn will shift the second equilibrium toward the free protonated form of the protein.

Additional investigations need to be performed to characterize the existence of subsequent steps in saposin C's membrane-binding process once the negative charge of its electrostatic surface has been reduced. NMR structural studies of human saposin C in the presence of SDS micelles are being performed in our laboratory to determine the three-dimensional structure of saposin C in a membrane-mimicking environment. This information will be important to identify conformational changes that saposin C may undergo by interacting with the membrane.

It has been previously suggested that Asn 22 (saposin C's glycosylation site) is not located close to the protein−membrane binding area (*18*), since no change in membrane-binding affinity or protein function have been observed between the glycosylated and the unglycosylated forms. Our structural data agree with this suggestion. Asn 22, located at the loop between helices I and II, is not close to the three clusters of Glu residues with elevated pK_a values, which according to our results are involved in the binding process. Additionally, Asn 22 side chain is solvent exposed and does not form any specific interactions with other residues. It is therefore unlikely that glycosylation will cause significant perturbations in saposin C's structure. Important electrostatic changes are not expected either, since they could modify the pK_a values of Glu residues, which would affect membrane binding.

Comparison of Saposin C's Structure with other Members of the Saposin-Fold Family and Implications for Different

Functionality. Several three-dimensional structures have been reported of proteins that share the saposin fold. All of these proteins bind to membranes or lipids. In contrast, although some have similar functions, others are functionally unrelated. In the majority of the cases the saposin fold is conserved, with minor differences in the arrangement of the helices and the short loops. Nevertheless, the electrostatic surfaces of these proteins are very different, ranging from positively to negatively charged. On the basis of a different electrostatic surface it is possible to expect different mechanisms of interaction with membranes that could account for functional diversity.

NK-lysin, a member of the saposin-fold family with tumorolytic and antibacterial properties, is supposed to form pores in membranes (*57*, *58*). The amino acid sequences of NK-lysin and saposin C are ~40% similar. The large difference between the structures of these two proteins is found in the electrostatic surface, since their backbone folds are very similar with a RMSD of 2.38 Å (Figure 9A). The NK-lysin surface is positively charged (Figure 4B). It contains a hydrophobic patch, that is suggested to be in closest contact to the membrane in the membrane-bound form, and a large number of positively charged residues that may form favorable interactions with negatively charged membranes (*57*, *58*). In contrast, saposin C's electrostatic surface is mainly negative (Figure 4A). While the binding of saposin C to membranes depends on pH, no data are available about the effect of pH on NK-lysin interaction with membranes. Furthermore, NK-lysin has an electrostatic surface that is very similar to those of membrane-disrupting proteins, bacteriocin AS-48 (*59*) and granulysin (*60*), whose structures resemble the saposin fold.

The plant specific domain of plant aspartic proteinase prophytepsin adopts the saposin fold (*61*) and is supposed to be involved in vacuolar transport mediated by membrane binding (*61*). Figure 4C shows that the electrostatic surfaces of the saposin-like domain in prophytepsin and that of saposin C are very different. Therefore, they are expected to interact with membranes differently.

Saposin B is another member of the saposin-fold family. In contrast to saposin C, saposin B solubilizes sphingolipids, acting as a carrier of the substrate to the enzyme responsible for its degradation (*62*). The crystal structure of saposin B differs from the so-called saposin fold. It consists of a homodimer with secondary structure very similar to that of saposin C but a very different arrangement of the helices (*63*) (Figure 9B).

This structural comparison highlights the possible implications that the protein electrostatic surface and the tertiary fold can have in the functional diversity and membrane binding properties of this family of proteins.

Implications for pH-Controlled Lipid Degradation in the Lysosome. It has been suggested that the binding of saposin C to artificial membranes at acidic pH values may be related to the fact that saposin C is a lysosomal protein, and that the pH in lysosomes tends to be acidic (*64*). Degradation of glycosphingolipids, the process in which saposin C is implicated, occurs in the acidic organelles of the cell (i.e., endosomes and lysosomes) (*65*). Saposin C is generated by proteolytic cleavage of its precursor in the late endosomes (*66*) and it has been found in the lysosomes, according to several studies on its subcellular localization (*6*, *66*−*68*).

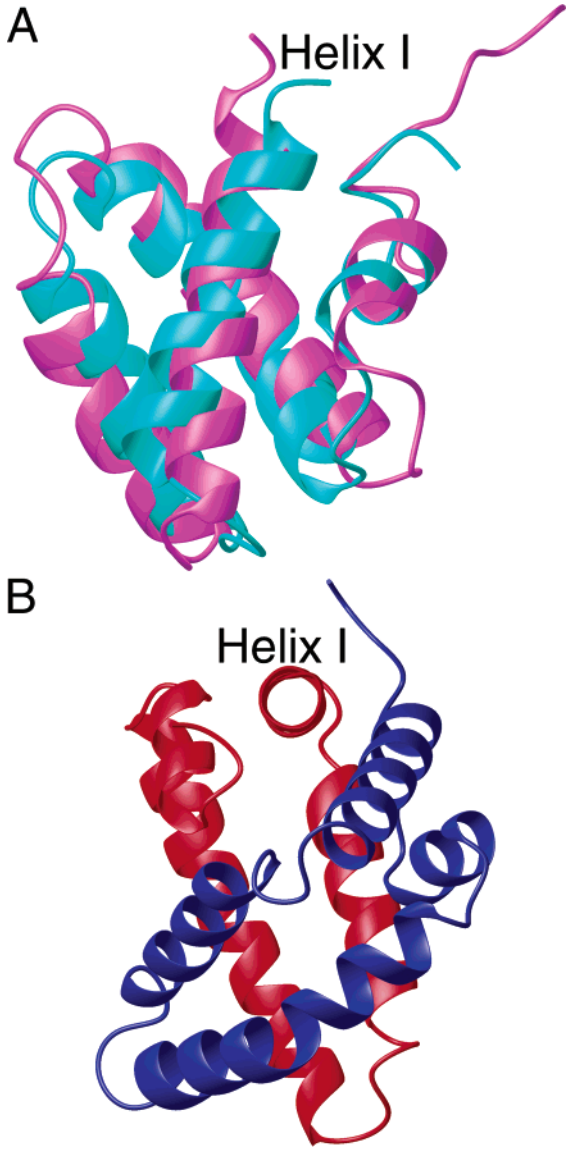

FIGURE 9: (A) Superposition of the ribbon diagrams representing the backbones of human saposin C (magenta) and NK-lysin (cyan). (B) Ribbon diagram representing the backbone of the dimeric structure of saposin B. The position of the dimer unit colored in red is equivalent to that of saposin C represented in the right-hand side of Figure 1A by matching the orientation of helix I. The different packing of the helices around helix I in saposin C and the saposin B dimer can be compared. Figure 9 was generated using the program MOLMOL (*82*).

These reports indicate that saposin C is associated with the lysosomal membrane, although it is also present in the lysosomal matrix. It has been mentioned that extractions of the protein in hypotonic medium resulted in the release of saposin C from cellular membranes apparently in a soluble form (*67*). This result is the first indication of the effect that solution conditions can have in the release of saposin C from the lysosomal membrane. We have found that saposin C can be released from the membranes by increasing the pH from acidic to neutral values, and that this process is reversibly controlled by pH. In addition, we have shown that changes in the net charge of the electrostatic surface of saposin C are responsible for its binding or its release from the membrane.

The pH of lysosomes ranges from ~4.5 to ~7.0 (*69*, *70*). The most common range is ~5.0−5.5 (*71*−*74*). Due to the

biogenesis of lysosomes (*75*, *76*) and/or to molecular processes taking place inside them (*77*), the pH value of an individual lysosome in a cell can vary with time (*69*, *77*) and also vary among the lysosomal population of the cell (*70*). For example, transient alkalinization could take place by the fusion of the lysosome with the less acidic endosome. This pH variability inside an individual lysosome can have important implications in sphingolipid degradation by regulating saposin C's binding to the lysosomal membrane. The pH-controlled reversibility of saposin C's binding to artificial membranes would imply a pH-controlled degradation of lipids, since binding of saposin C to the membrane is key to the activation of the lysosomal hydrolase glucocerebrosidase (*8*, *10*, *11*). In vivo studies concerning a glucocerebrosidase mutant frequently encountered in Gaucher disease, indicate that intra-lysosomal pH has a critical effect in the catalytic efficiency of the enzyme (*78*). This result can be due to the effect of pH on the enzyme itself or on saposin C. Additionally, other physiological disorders related to lipid accumulation have been associated with elevated lysosomal pH values, even though the lysosomal hydrolases that participate in lipid hydrolysis appear to function normally (*79*, *80*). These studies also suggest that pH plays a very important role in lipid degradation inside the lysosome.

ACKNOWLEDGMENT

We are grateful to Victor Muñoz for interesting suggestions and careful reading of the manuscript, and to James Gruschus for useful advice and assistance. We also thank James A. Ferretti for the careful reading of the manuscript. We thank Cheryl Hawkins for providing some double-labeled saposin C.

REFERENCES

1. O'Brien, J. S., and Kishimoto, Y. (1991) *FASEB J. 5*, 301−308.
2. Schnabel, D., Schroder, M., and Sandhoff, K. (1991) *FEBS Lett. 284*, 57−59.
3. Horowitz, M., and Zimran, A. (1994) *Hum. Mutat. 3*, 1−11.
4. Munford, R. S., Sheppard, P. O., and O'Hara, P. J. (1995) *J. Lipid. Res. 36*, 1653−1663.
5. Ito, K., Takahashi, N., Takahashi, A., Shimada, I., Arata, Y., O'Brien, J. S., and Kishimoto, Y. (1993) *Eur. J. Biochem. 215*, 171−179.
6. Sano, A., Hineno, T., Mizuno, T., Kondoh, K., Ueno, S., Kakimoto, Y., and Inui, K. (1989) *Biochem. Biophys. Res. Commun. 165*, 1191−1197.
7. Vaccaro, A. M., Ciaffoni, F., Tatti, M., Salvioli, R., Barca, A., Tognozzi, D., and Scerch, C. (1995) *J. Biol. Chem. 270*, 30576−30580.
8. Salvioli, R., Tatti, M., Ciaffoni, F., and Vaccaro, A. M. (2000) *FEBS Lett. 472*, 17−21.
9. Weiler, S., Kishimoto, Y., O'Brien, J. S., Barranger, J. A., and Tomich, J. M. (1995) *Protein Sci. 4*, 756−764.
10. Vaccaro, A. M., Tatti, M., Ciaffoni, F., Salvioli, R., Barca, A., and Scerch, C. (1997) *J. Biol. Chem. 272*, 16862−16867.
11. Wilkening, G., Linke, T., and Sandhoff, K. (1998) *J. Biol. Chem. 273*, 30271−30278.
12. Sano, A., and Radin, N. S. (1988) *Biochem. Biophys. Res. Commun. 154*, 1197−1203.
13. Weiler, S., Carson, W., Lee, Y., Teplow, D. B., Kishimoto, Y., O'Brien, J. S., Barranger, J. A., and Tomich, J. M. (1993) *J. Mol. Neurosci. 4*, 161−172.
14. Qi, X., Leonova, T., and Grabowski, G. A. (1994) *J. Biol. Chem. 269*, 16746−16753.
15. Morimoto, S., Martin, B. M., Yamamoto, Y., Kretz, K. A., O'Brian, J. S., and Kishimoto, Y. (1989) *Proc. Natl. Acad. Sci. U.S.A. 86*, 3389−3393.
16. Hiraiwa, M., Soeda, S., Martin, B. M., Fluharty, A. L., Hirabayashi, Y., O'Brian, J. S., and Kishimoto, Y. (1993) *Arch. Biochem. Biophys. 303*, 326−331.
17. Rijnboutt, S., Aerts, H. M. F. G., Geuze, H. J., Tager, J. M., and Strous, G. J. (1991) *J. Biol. Chem. 266*, 4862−4868.
18. Tatti, M., Salvioli, R., Ciaffoni, F., Pucci, P., Andolfo, A., Amoresano, A., and Vaccaro, A. M. (1999) *Eur. J. Biochem. 263*, 486-494.
19. Hansen, M. R., Mueller, L., and Pardi, A. (1998) *Nat. Struct. Biol. 5*, 1065−1074.
20. Bax, A., and Grzesiek, S. (1993) *Acc. Chem. Res. 26*, 131−138.
21. Ottiger, M., Delaglio, F., and Bax, A. (1998) *J. Magn. Reson. 131*, 373−378.
22. Ottiger, M., Delaglio, F., Marquardt, J. L., Tjandra, N., and Bax, A. (1998) *J. Magn. Reson. 134*, 365−369.
23. Delaglio, F., Grzesiek, S., Vuister, G. W., Zhu, G., Pfeifer, J., and Bax, A. (1995) *J. Biomol. NMR 6*, 277−293.
24. Garrett, D. S., Powers, R., Gronenborn, A. M., and Clore, G. M. (1991) *J. Magn. Reson. 95*, 214−220.
25. Marion, D., Ikura, M., Tschudin, R., and Bax, A. (1989) *J. Magn. Reson. 85*, 393−399.
26. Barbato, G., Ikura, M., Kay, L. E., Pastor, R. W., and Bax, A. (1992) *Biochemistry 31*, 5269−5278.
27. Piotto, M., Saudek, V., and Sklenar, V. (1992) *J. Biomol. NMR 2*, 661−665.
28. Bax, A., and Pochapsky, S. S. (1992) *J. Magn. Reson. 99*, 638−642.
29. Grzesiek, S., and Bax, A. (1993) *J. Biomol. NMR 3*, 185−204.
30. Peng, J. W., Thanabal, V., and Wagner, G. (1991) *J. Magn. Reson. 95*, 421−427.
31. Grzesiek, S., and Bax, A. (1993) *J. Am. Chem. Soc. 115*, 12593−12594.
32. Brunger, A. T. (1993) *X-PLOR Version 3.1: A System for X-ray Crystallography and NMR*, Yale University Press, New Haven, Connecticut.
33. Tjandra, N., Omichinski, J. G., Gronenborn, A., Clore, M. G., and Bax, A. (1997) *Nat. Struct. Biol. 4*, 732−738.
34. Clore, M. G., Gronenborn, A. M., and Bax, A. (1998) *J. Magn. Reson. 133*, 216−221.
35. Cornilescu, G., Delaglio, F., and Bax, A. (1999) *J. Biomol. NMR 13*, 289−302.
36. Yamazaki, T., Nicholson, L. K., Torchia, D. A., Wingfield, P., Stahl, S. J., Kaufman, J. D., Eyerman, C. J., Hofge, C. N., Lam, P. Y. S., Ru, Y., Jadhav, P. K., Chang, C.-H., and Weber, P. C. (1994) *J. Am. Chem. Soc. 116*, 10791−10792.
37. Wishart, D. S., Sykes, B. D., and Richards, F. M. (1991) *J. Mol. Biol. 222*, 311−333.
38. Wuthrich, K. (1986) *NMR of Proteins and Nucleic Acids*, Wiley, New York.
39. Wishart, D. S., Bigam, C. G., Holm, A., Hodges, R. S., and Sykes, B. D. (1995) *J. Biomol. NMR 5*, 67−81.
40. Vaccaro, A. M., Salvioli, R., Barca, A., Tatti, M., Ciaffoni, F., Maras, B., Siciliano, R., Zappacosta, F., Amoresano, A., and Pucci, P. (1995) *J. Biol. Chem. 270*, 9953−9960.
41. Peng, J. W., and Wagner, G. (1994) *Methods Enzymol. 239*, 563−596.
42. Lipari, G., and Szabo, A. (1982) *J. Am. Chem. Soc. 104*, 4546−4559.
43. Lipari, G., and Szabo, A. (1982) *J. Am. Chem. Soc. 104*, 4559−4570.
44. Muller, L. (1979) *J. Am. Chem. Soc. 101*, 4481−4484.
45. Bodenhausen, G., and Ruben, D. J. (1980) *Chem. Phys. Lett. 69*, 185−189.
46. Bax, A., Ikura, M., Kay, L. E., Torchia, D. A., and Tschudin, R. (1990) *J. Magn. Reson. 86*, 304−318.
47. Shuker, S. B., Hajduk, P. J., Meadows, R. P., and Fesik, S. W. (1996) *Science 274*, 1531−1534.
48. Delepierre, M., Dobson, C. M., Karplus, M., Poulsen, F. M., States, D. J., and Wedin, R. E. (1987) *J. Mol. Biol. 197*, 111−130.
49. Honig, B., and Nicholls, A. (1995) *Science 268*, 1144−1149.
50. Perez-Canadillas, J. M., Campos-Olivas, R., Lacadena, J., Martinez del Pozo, A., Gavilanes, J. G., Santoro, J., Rico, M., and Bruix, M. (1998) *Biochemistry 37*, 15865−15876.
51. Chen, H. A., Pfuhl, M., McAlister, M. S. B., and Driscoll, P. C. (2000) *Biochemistry 39*, 6814−6824.
52. Chen, H. A., Pfuhl, M., and Driscoll, P. C. (2002) *Biochemistry 41*, 14680−14688.
53. Damberg, P., Jarvet, J., and Graslund, A. (2001) *Methods Enzymol. 339*, 271−285.

54. Lane, A. N., and Lefevre, J.-F. (1994) *Methods Enzymol. 239*, 596−619.
55. Moncelli, M. R., Becucci, L., and Guidelli, R. (1994) *Biophys. J. 66*, 1969−1980.
56. Tsui, F. C., Ojcius, D. M., and Hubbell, W. L. (1986) *Biophys. J. 49*, 459−468.
57. Liepinsh, E., Andersson, M., Ruysschaert, J.-M., and Otting, G. (1997) *Nat. Struct. Biol. 4*, 793−795.
58. Ruysschaert, J.-M., Goormaghtigh, F., Homble, F., Andersson, M., Liepinsh, E., and Otting, G. (1998) *FEBS Lett. 425*, 341−344.
59. Gonzalez, C., Langdon, G., Bruix, M., Galvez, A., Valdivia, E., Maqueda, M., and Rico, M. (2000) *Proc. Natl. Acad. Sci. U.S.A. 97*, 11221−11226.
60. Anderson, D. H., Sawaya, M. R., Cascio, D., Ernst, W., Krensky, A., and Eisenberg, D. (2003) *J. Mol. Biol. 325*, 355−365.
61. Kervinen, J., Tobin, G. J., Costa, J., Waugh, D. S., Wlodawer, A., and Zdanov, A. (1999) *EMBO J. 18*, 3947−3955.
62. Furst, W., and Sandhoff, K. (1992) *Biochim. Biophys. Acta Lipids Lipid Metab. 1126*, 1−16.
63. Ahn, V. E., Faull, K. F., Whitelegge, J. P., Fluharty, A. L., and Prive, G. G. (2003) *Proc. Natl. Acad. Sci. U.S.A. 100*, 38−43.
64. Vaccaro, A. M., Salvioli, R., Tatti, M., and Ciaffoni, F. (1999) *Neurochem. Res. 24*, 307−314.
65. Bierfreund, U., Kolter, T., and Sandhoff, K. (2000) *Methods Enzymol. 311*, 255−276.
66. Vielhaber, G., Hurwitz, R., and Sandhoff, K. (1996) *J. Biol. Chem. 271*, 32438−32446.
67. Chiao, Y.-B., Chambers, J. P., Glew, R. H., Lee, R. E., and Wenger, D. A. (1978) *Arch. Biochem. Biophys. 186*, 42−51.
68. Paton, B. C., Hughes, J. L., Harzer, K., and Poulos, A. (1990) *Eur. J. Cell Biol. 51*, 157−164.
69. Ogloblina, T. A., Litinskaia, L. L., and Veksler, A. M. (1987) *Vopr. Med. Khim. 33*, 56−59.
70. Yamashiro, D. J., and Maxfield, F. R. (1987) *J. Cell. Biol. 105*, 2723−2733.
71. Moriyama, Y., Maeda, M., and Futai, M. (1992) *FEBS Lett 302*, 18−20.
72. Tsuboi, M., Harasawa, K., Izawa, T., Komabayashi, T., Fujinami, H., and Suda, K. (1993) *J. Appl. Physiol. 74*, 1628−1634.
73. Wan, F. Y., and Zhang, G. J. (2002) *Arch Biochem. Biophys. 402*, 268−274.
74. Chen, C.-S. (2002) *BMC Cell Biol. 3*, 1471−2121.
75. Storrie, B., and Desjardins, M. (1996) *BioEssays 18*, 895−903.
76. Bucci, C., P., T., Nicoziani, P., McCarthy, J., and van Deurs, B. (2000) *Mol. Biol. Cell 11*, 467−480.
77. Butor, C., Griffiths, G., Aronson, N. N., and Varki, A. (1995) *J. Cell Sci. 108*, 2213−2219.
78. van Weely, S., ven den Berg, M., Barranger, J. A., Sa Miranda, M. C., Tager, J. M., and Aerts, J. M. (1993) *J. Clin. Invest. 91*, 1167−1175.
79. Holopainen, J. M., Saarikoski, J., Kinnunen, P. K., and Jarvela, I. (2001) *Eur. J. Biochem. 268*, 5851−5856.
80. Bach, G., Chen, C.-S., and Pagano, R. E. (1999) *Clin. Chim. Acta 280*, 173−179.
81. Laskowski, R. A., Rullman, J. A. C., MacArthur, M. W., Kaptein, R., and Thornton, J. M. (1996) *J. Biomol. NMR 8*, 477−486.
82. Koradi, R., Billeter, M., and Wuthrich, K. (1996) *J. Mol. Graphics 14*, 51−55.

BI0301338